Journal of Analytical and Applied Pyrolysis 115 (2015) 203–213

Contents lists available at ScienceDirect

Journal of Analytical and Applied Pyrolysis

journal homepage: www.elsevier.com/locate/jaap

Fast pyrolysis of lignin-coated radiata pine

Andrew Moore [a], Sunkyu Park [a], Cristina Segura [b], Marion Carrier [b,*]

[a] Department of Forest Biomaterials, North Carolina State University, Raleigh, NC 27695, United States
[b] Centre for Technological Development-UDT, Parque Industrial Coronel, Concepción, Chile

ARTICLE INFO

Article history:
Received 26 May 2015
Received in revised form 20 July 2015
Accepted 21 July 2015
Available online 28 July 2015

Keywords:
Lignin-coating
Biomass
Fast pyrolysis

ABSTRACT

A new coating preparative method of the *Pinus radiata* feedstock was used to process a mixture of Acetocell lignin and sawdust prepared at different mass ratios of lignin to sawdust, 1:18 (LI_{20}) and 1:7 (LI_{40}) to overcome feeding issues into a fluidized bed pyrolysis reactor.

The coated materials were structurally characterized by using spectrometric and microscopic techniques, which respectively confirmed the presence of saturated aliphatic and oxygenated side chains in the isolated lignin and the formation of a boundary layer around the woody biomass particles. The fast pyrolysis of the coated materials at 540 °C led to the decrease of both total liquid and organic yields and to the substantial increase of reactive water yield. Like yields, the addition of the technical lignin affected the product composition of fast pyrolysis bio-oil. These changes were both related to the oxygenated aliphatic nature of the lignin side-chains and to the thickness of the coating layer.

This new preparation technique of the feedstock overcomes the technical barriers associated with the feeding of thermoset polymers into a bubbling fluidized bed reactor, without modifying its initial design; and enhanced the production of the phenolic rich fraction by controlling the thickness of the coating.

1. Introduction

The valorization of secondary streams such as extracted tannins and Acetosolv lignin from *Pinus radius* is a key issue in the development of lignocellulosic biorefineries [1]. In the last decade, an intensive research activity was carried out on the valorization of technical lignins [2–5], while the valorization of extracted tannins has been studied more recently [6,7].

Urged by a need of diversifying its pool of technologies to produce renewable energy, Chile with its natural abundance of woody biomass supported the implementation of fast pyrolysis in the country. A fast pyrolysis process using a three-stage fluidized bed reactor system with a feed capacity of 10 kg/h was developed at the Unidad de Desarrollo Tecnológico, UDT [8]. Fast pyrolysis, a thermochemical process that converts biomass into a useful liquid product, is currently of particular interest for fuel and chemical production [9]. The valorization of technical lignins such as acid-extracted and Organosolv lignins are often considered due to their low sulfur content [10,11], being a perfect candidate for the establishment of a cleaner valorization process. Previous works have proved the viability and feasibility of converting these lignins into a value-added chemicals source by showing the occurrence of high-value components (e.g., hydroxyacetaldehyde, acids, and phenolic monomers) in fast pyrolysis bio-oil obtained from Acetosolv or Kraft lignin [12], or Organosolv lignin [13,14]. The concentration of these organic compounds depends on the nature of the lignocellulosic feedstocks [15], whose chemistry was altered during the extraction process [11]. However, the conventional fast pyrolysis of these extracted biopolymers presents numerous technical issues, in particular feeding problems due to their low fusion point, bed agglomeration, and low yield of highly oxygenated liquids [5,7,16]. To overcome these technical barriers, several alternative pyrolysis modifications have been attempted, such as the co-feeding with alkaline catalyst or the use of a catalytic bed. For example, the addition of CaO helped decrease the oxygen content of bio-oil by reducing the concentration of levoglucosan in favor of the acetol [17]. The combined use of CaO and an olivine bed appeared to be beneficial, as it displayed a high liquid yield, 32 wt%, and favored the depolymerization of Acetocell lignins [18]. More recently, Li et al. [19] proposed the use of activated lignin bed to pyrolyze Kraft lignin in order to improve the bio-oil's quality.

In this study, the coating of biomass particles with isolated lignin was proposed as an alternative method to the addition of catalysts. To fully understand the role of the coating preparation on product distribution and pyrolysis reactions, this study used both spectrometric and chromatographic techniques, ^{13}C NMR and GC–MS,

* Corresponding author.
E-mail addresses: m.carrier@udt.cl, marion_carrier@msn.com (M. Carrier).

http://dx.doi.org/10.1016/j.jaap.2015.07.017
0165-2370/

to respectively analyze the overall pyrolysis bio-oil and quantify its key-products obtained from raw biomass and coated materials pyrolysis degradation.

2. Materials and methods

2.1. Materials and preparation

2.1.1. Feedstocks

Pinus radiata D. Don sawdust was provided by BSQ Ltda, a forest company located in Concepción (Chile). The woody material was sieved to obtain a particle size in the range of 0.5–1.5 mm. The moisture content (MC) of the woody material was maintained at 10 wt.%.

The acetic acid-extracted lignin (Acetosolv lignin) was prepared from the same *P. radiata* wood chips using an adaptation of the so-called Acetocell process [20]. The woody material was delignified using an 87 wt% acetic acid solution at 185 °C for 2 h. The dissolved lignin was precipitated by diluting the spent pulping liquor with water. The filtered lignin was washed with water multiple times. Since the pulping method is sulfur and sodium free, the Acetosolv lignin has low ash and contains almost no covalently bound sulfur in comparison to others extracted lignin originating from the kraft process [11].

2.1.2. Coated feedstocks

A preparation method was developed to produce the coated feedstock with a uniform distribution of lignin. A solvent mixture of acetone (99.5%, Winkler) and water, four parts to one respectively, was utilized to fully dissolve the acetic-extracted lignin (up to 0.2 g/mL). A liquor to wood ratio of 8:1 was used to allow the slurry to be evenly mixed. The lignin was fully dissolved in the acetone/water mixture in 10 min with vigorous mixing (4000 rpm) via a mechanical stirrer. The pine powder was then added slowly over 10 min to ensure a uniform mixture and allowed to mix for 4 h. After mixing, the sample was left in a beaker, then covered, and allowed to soak overnight for further impregnation by lignin. The sample was then placed into a pan and placed in a fume hood to allow the solvent to evaporate, and then oven dried at 45 °C for 2 h, and finally allowed to air dry for 48 h. The coated biomass was then sieved to the original 250–600 μm particle size.

2.2. Fast pyrolysis processing

The fast pyrolysis (FP) plant (Fig. 1) can be divided into four sections: the biomass-feeding unit, the cylindrical furnace housing the bubbling fluidized bed reactor, one hot-gas filter as separation stage, and the condensation chain. The biomass feeding unit consisted of a hopper with a screw feeder, which introduced biomass (particle size 250–600 μm) at a feed rate of 0.1 ± 0.03 kg/h into the reactor. The hopper was maintained at a slight N_2 overpressure (±0.02 bar gauge, gas flow rate of 6 L/min) to prevent hot gas and product vapor pushing back from the reactor into the feeding system. A quartz bed was used as the heat carrier inside the reactor and fluidized using a N_2 gas flow rate of 9 L/min. Pyrolysis product vapors/aerosols and solid particles left the furnace via a heated pipe (maintained at 400 °C to prevent undesired intermediate condensation) before entering the hot gas filter at 400 °C. Once separated from solid particles, the aerosols/vapors underwent a condensation stage, that consisted of a water-cooling tower at 4 °C followed by an electrostatic precipitator set to 15 kV.

The bio-oil, product of interest, was collected from the condenser tower and precipitator and thus consisted of two single phases corresponding to the BOC and BOP fractions. The char product was recovered from the hot-filter pot, while the non-condensable gases were purged to the atmosphere. Experimental runs were duplicated at 540 °C with a running time between 25 and 65 min.

All product yields (Y_{char}, $Y_{bio\text{-}oil}$, $Y_{organics}$, and $Y_{pyrolytic\ water}$) reported here were calculated on a dry mass basis (db, wt%) of the initial and dried biomass feed, $m_{biomass}(1 - MC_0)$, as indicated by Eqs. (1)–(4). The bio-oil yield represents the total liquid product yield correcting for initial feed water content.

$$Y_{char}(\text{db, wt.\%}) = \frac{m_{char}(1 - MC_{char})}{m_{biomass}(1 - MC_0)} \times 100 \quad (1)$$

$$Y_{bio\text{-}oil}(\text{db, wt.\%}) = \frac{m_{bio\text{-}oil} - m_{biomass} \times MC_0}{m_{biomass}(1 - MC_0)} \times 100 \quad (2)$$

$$Y_{organics}(\text{db, wt.\%}) = \frac{m_{bio\text{-}oil}(1 - MC_{bio\text{-}oil})}{m_{biomass}(1 - MC_0)} \times 100 \quad (3)$$

$$Y_{pyrolyticwater}(\text{db, wt.\%}) = \frac{m_{bio\text{-}oil} \times MC_{bio\text{-}oil} - m_{biomass} \times MC_0}{m_{biomass}(1 - MC_0)} \times 100 \quad (4)$$

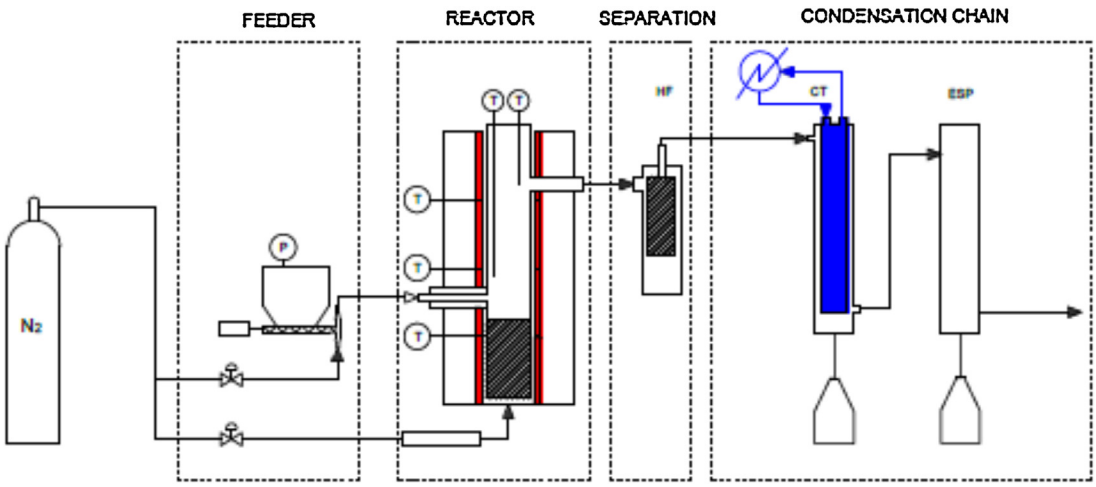

Fig. 1. Fast pyrolysis set-up showing the four sections.

where m_{char}, $m_{bio\text{-}oil}$, and $m_{biomass}$ are respectively the mass of recovered char, bio-oil and initial biomass. The gas yield was calculated by difference.

2.3. Analyses

2.3.1. Feedstock

Ultimate and proximate analyses were conducted on both feedstocks using respectively an elemental analyzer (Perkin Elmer 2400 Series II CHNS/O system) and a thermogravimetric analyzer (TA instruments Q500) using the ASTM E1131 standard procedure.

The surface of feedstock was analyzed using a single reflection attenuated total reflectance (ATR) FT-IR technique performed by a Platinum ATR Alpha instrument. A total of 24 scans between 4800 and 400 cm^{-1} were averaged at intervals of 4 cm^{-1}. The software OPUS (Version 7) was used to normalize and display the spectra.

Compositional analysis was performed using a modified NREL method, which has been described elsewhere [21]. The determination of water, ethanol and hexane extractives within the raw *P. radiata* was carried out following the NREL Laboratory Analytical procedure [22].

An oven-dried sample mass of 0.1 g of 250–400 μm biomass was hydrolyzed with 72 wt% H_2SO_4 (Sigma–Aldrich) for 2 h, then diluted to 3% before being autoclaved at 120 °C for 1.5 h. Hydrolysate was filtered and the liquid was analyzed by HPLC system (Agilent 1200, Agilent, Santa Clara, CA, USA) and UV–Vis spectrophotometer (Lambda XLS, Perkin Elmer, Waltham, MA, USA) for sugar and lignin analysis, respectively. The sugars, glucose, xylose, and galactose were detected and measured by ways of calibration curves obtained from standards, glucose (>99.5%, Sigma–Aldrich), xylose (>99%, Sigma–Aldrich), and galactose (>99%, Sigma–Aldrich). The solids were oven-dried at 105 °C and weighed to determine the insoluble lignin fraction.

The chemical structure of the lignin was determined by ^1H NMR after complete acetylation of the material. The protocol of acetylation was an adaptation of the one proposed by Fernandez-Costas et al. [23]. Volumes of 5 mL of acetyl anhydride (99.2%, Winkler) and 5 mL of pyridine (99.7%, Winkler) were added to 52.5 mg of lignin in a dry acetylation vial, which was sealed and constantly stirred at 37 °C for 48 h. A volume of 20 mL of cold distilled water was added to the mixture to remove the excess of pyridine and acetyl anhydride and subsequently precipitate the lignin. After the first centrifugation step at 15,000 rpm for 4 min using an Eppendorf system (Model 5702), two additional clean-up steps were performed. The contents of the vial were finally dried at 40 °C for 48 h and milled with an agate mortar and pestle. Acetylated and non-acetylated lignins (~25 mg) were dissolved in 750 mL of deuterated methanol CD_3OD-*d4* (99.8%, Merck). The spectra were collected on a Bruker Avance DSZ 400 MHz spectrometer at 23.5 °C, equipped with a BRUKER 5 mm PABBI 1 H/D-BB Z-GRD liquid probe with a flip angle of 30°. The number of scan was 16 with an acquisition time of 6.3 s. Spectra were processed with Bruker TopSpin 3.1.

Finally, pictures of coated particles were taken using a scanning electron microscope (SEM) micrograph JEOL (JSM-6010LA) equipment using a magnification range of 22–2500 with a resolution of 0.28 nm.

2.3.2. Bio-oil

The water content of liquid fractions was determined using a Mettler Toledo V20 volumetric KF Titrator (ASTM E871) using the CombiTitrant 5 one-component reagent for volumetric Karl-Fisher titration (Merck) as titration reactant and dried methanol (max 0.003% H_2O, Merck) as titration solvent.

Chemical functional groups of char and tarry fractions were determined using nuclear magnetic resonance (NMR), on a Bruker Avance DSZ 400 MHz spectrometer. The analysis of ^{13}C NMR was acquired using ~140.0 mg tarry oil dissolved in 900 μL DMSO-d_6 (99.8%, Merck) or ~100.0 mg of char dissolved in 900 μL DMSO-d_6 employing an inverse gated decoupling pulse sequence, 90° pulse angle, a pulse delay of 5 s for tarry oils, and 12 s for char. The ^{13}C NMR spectra were acquired with a 90° pulse duration of 2.4 μs, and a sweep width of 25,000 Hz and 30,000 Hz for liquids and chars. Spectra were processed using Bruker TopSpin 3.1. The chemical shift values were calibrated on the solvent peak. The ^{13}C NMR chemical shift assignment was determined based on previous works of Ben et al. [24].

The GC–MS analyses were performed using a Hewlett Packard GC system (Model HP 6890Series) and a Hewlett Packard Mass Selective detector (Model 5973). A column HP-5 60 m × 0.25 mm with a film thickness of 0.25 μm and operating conditions were based on following past procedures [25]. The heating program was an initial hold at 45 °C for 4 min, followed by a ramp to 280 °C at 3 °C/min, and finally held at 280 °C for 15 min. An aliquot of 0.2 g of bio-oil and 1 mL of internal standard (Fluoranthene, 98%, Aldrich) were added to a 10 mL volumetric flask that was completed with acetone (GC grade, Sigma–Aldrich) filtered through a 0.2 μm PTFE filter (Rephile). The volume injection was 1 μL and maintained by an autosampler. The mass spectrometer (MS) detector was used with a standard electron impact ionization chamber set at 70 eV with a temperature of 200 °C. The ions formed were separated via a quadrupole according their mass-to-charge (m/z) ratio in the range of 30–250 Da. Peaks were identified by the 2008 NIST library.

3. Results and discussion

3.1. Feedstocks characterization

The initial characterization of the feedstocks was important to appreciate the efficiency of the coating method and the possible chemical and/or physical changes. The compositional analysis showed in Table 1 indicates that the lignin content was increased systematically and effectively. The starting biomass contained 32.78 wt% of native lignin, which was increased to 38.30 wt% in LI_{20} and to 46.83 wt% in LI_{40}; thus corresponding respectively to an increase of 17% (LI_{20}) and 43% (LI_{40}) in lignin mass within the coated materials. The moisture content remained constant for all samples between 3.97% and 5.61 wt% meaning the samples were effectively dried prior to being pyrolyzed. Although both ash content of virgin biomasses are low, 0.68 and 0.54 wt% for pine and the isolated lignin respectively, a slight increase in ash content was observed for the coated preparations, 0.81 wt% for LI_{20} and 1.12 wt% for LI_{40}. This result was attributed to the impurities present in the acetone solvent used during the preparation.

The chemical composition indicates that 7.74 wt% of the dry mass cannot be accounted from the analysis results. Similar problems with respect to unclosed or overestimated mass balance were experienced in different studies [26,27]. In some cases, authors attributed those deviations to unidentified or lost materials after acid hydrolysis of the biomass feedstock and/or the inaccuracy of the isolation method [28,29]. In our case, the lignocellulose distribution falls within the literature range and the unclosed mass balance can be partially attributed to the fact that we did not report the concentration of arabinose nor mannose.

Lignin together with hemicelluloses and cellulose provide the lignocellulose biomass with a large and diverse distribution of functional groups. Although ATR–FTIR does not allow an accurate quantification of the functional groups [30], this technique can be used as qualitative screening. Clear spectral differences between feedstocks were observed in the regions of 3700–2700 and 1800–500 cm^{-1} (Fig. 2). In the case of the isolated lignin, the respective strong bands at 1714, 1597, 1269 cm^{-1}, 1225 and

Table 1
Compositional and physico-chemical properties of feedstock.

	Pinus radiata	LI_{20}	LI_{40}	Acetosolv lignin
Moisture content	5.24 ± 1.37	3.97 ± 1.08	5.61 ± 1.42	4.74 ± 0.72
Compositional analysis (wt%)				
Carbohydrates	47.54 ± 1.25	41.40 ± 0.21	36.32 ± 0.58	3.77 ± 0.26
Glucan	43.34 ± 1.09	37.87 ± 0.16	33.46 ± 0.53	4.00 ± 0.23
Xylan	3.48 ± 0.08	3.04 ± 0.09	2.26 ± 0.07	0.00 ± 0.00
Galactose	0.72 ± 0.08	0.48 ± 0.07	0.24 ± 0.01	0.00 ± 0.04
Lignin	32.78 ± 0.74	38.30 ± 0.47	46.83 ± 1.40	97.19 ± 0.29
Acid Insoluble Residue (AIR)	32.23 ± 0.72	37.67 ± 0.45	45.87 ± 1.30	95.11 ± 0.17
Acid Soluble Lignin (ASL)	0.55 ± 0.02	0.63 ± 0.02	0.96 ± 0.10	2.08 ± 0.12
Extractives				
Hexane	0.95 ± 0.03			
Water	2.91 ± 0.08			
Ethanol	1.95 ± 0.11			
Ash	0.89	0.80	1.15	0.56
Mass balance	92.26	84.47	89.91	106.26
Ultimate analysis (db, wt%)				
C	48.18 ± 0.92	48.55 ± 0.20	51.37 ± 0.41	65.98 ± 0.11
H	5.61 ± 0.10	5.76 ± 0.37	5.44 ± 0.34	5.52 ± 0.38
N	0.07 ± 0.02	0.07 ± 0.02	0.07 ± 0.03	0.11 ± 0.01
O	49.74 ± 0.84	46.64 ± 0.30	44.84 ± 0.48	30.22 ± 0.54
Proximate analysis (db, wt%)				
VM	94.70	84.25	78.37	59.58
FC	4.38	14.93	20.48	39.87
AC	0.92	0.82	1.15	0.55

1127 cm^{-1} that are respectively assigned to the C=O stretching, aromatic skeletal vibration, combined C—O and C—C stretch and the aromatic C—H in-plane deformation in the guaiacyl ring, are characteristic of the coniferyl alcohol unit of softwood lignin [31]. In addition, the bands centered at 1454 cm^{-1} and 2850 cm^{-1} corresponding respectively to the CH deformation –OCH_3 aromatic and stretching vibration of C—H assigned to the OCH_3 confirmed that numerous methoxy groups that belong originally to the guaiacol (G) unit remained in large proportion after the hydrolysis [31].

The efficiency of the acid hydrolysis of lignin was confirmed by two observations. Firstly, the presence of intense peaks at 1714 cm^{-1} and 1366 cm^{-1} attributed to the respective presence of carbonyl and hydroxyl groups indicates the cleavage of the aryl–ether bonds [32]. Secondly, the absence of the band centered at 1315 cm^{-1} indicates that carbohydrates have been efficiently removed and their content remained low, 2.08 wt% (Table 1).

If the ATR–FTIR analysis qualitatively suggested the presence of side-chains with the detection of carbonyl groups, the use of ^1H NMR analysis is a more suitable technique to determine the type of protons within the structure of the isolated lignin. Signal assignment for ^1H NMR were adopted from the early work of Tejado et al. [32]. The acetylation of the lignin helped to reveal much defined proton signals in particular in the regions 9.0–6.0 and 3.0–0.9 ppm (Fig. 3). Although the ^1H NMR spectrum of the non-acetylated lignin indicates that the feedstock naturally contains aromatic and aliphatic acetyl groups (Fig. 3b), the upgraded signals

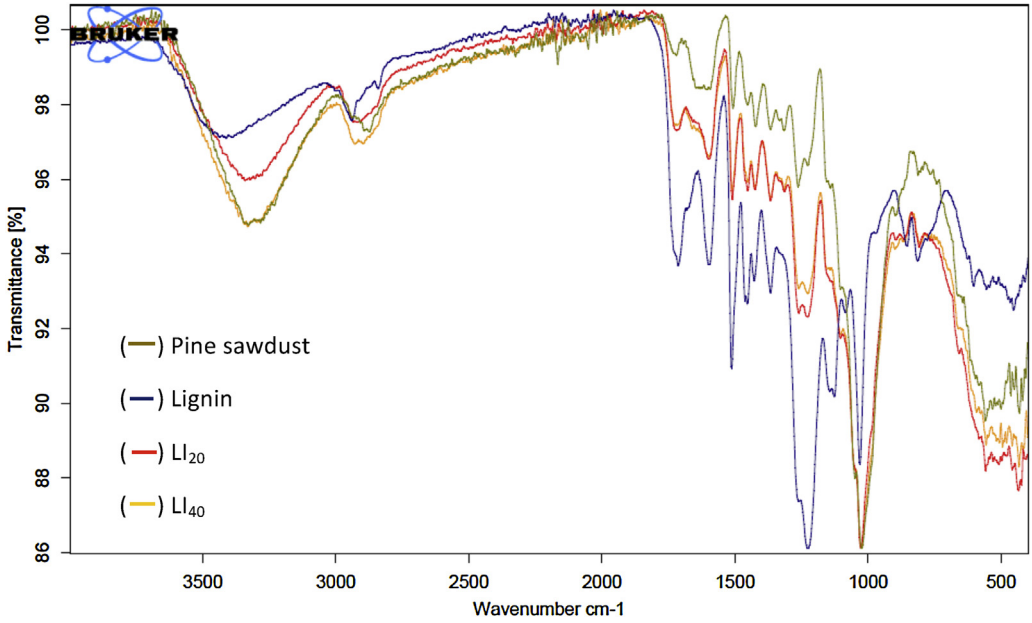

Fig. 2. ATR–FTIR spectra of raw and coated materials.

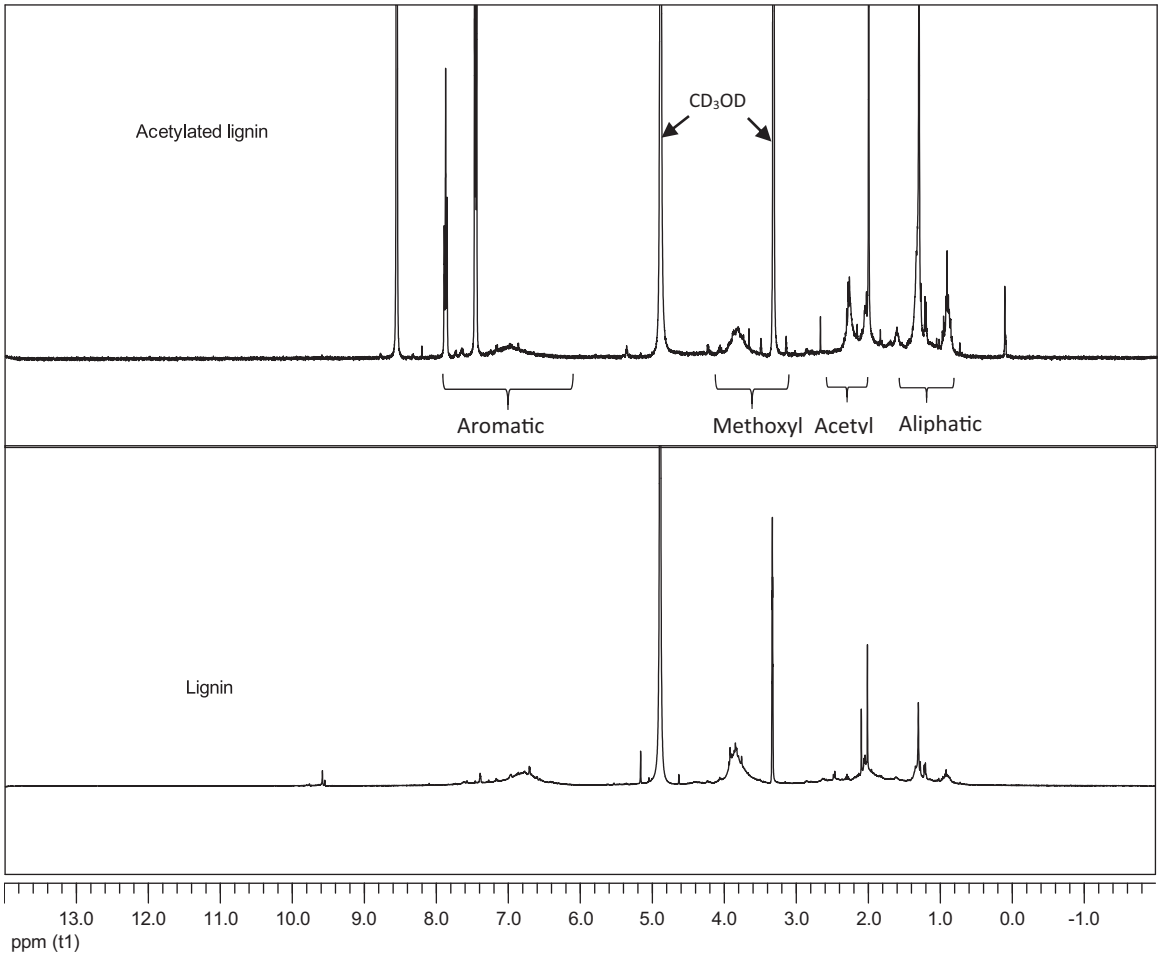

Fig. 3. ^{1}H NMR spectra of (a) the acetylated and (b) non-acetylated lignins with the following signal assignments: 10.0–9.7 ppm for H in benzaldehyde units, 8.0–6.0 ppm for aromatic H in sinapyl (S) and G units, 4.2–3.1 ppm for methoxyl H, 2.5–2.2 ppm for H in aromatic acetates, 2.2–1.9 for H in aliphatic acetates and 1.5–0.8 ppm for aliphatic H.

in the acetyl region (2.5–1.9 ppm) of the acetylated lignin spectrum (Fig. 3a) allowed the determination of the relative distribution between original OH groups [33]. The ratio of normalized areas between the hydrogens in aromatic acetates and the hydrogens in aliphatic acetates, 5:15, confirms the predominance of aliphatic –OH groups (α-OH, γ-OH and β-OH) and thus the existence of long side-aliphatic oxygenated chains.

Finally, the use of thermogravimetric analysis helped us to reveal the main features of the thermal degradation behavior for the raw and coated materials. Dynamic measurements indicated that the thermal stability of LI_{20} remained the same than that of pine starting to degrade at 180 °C, whereas the initial degradation temperature of LI_{40} was decreased to 145 °C. This was attributed to the larger addition of lignin that starts to degrade at 126 °C (Fig. 4). The maximum temperature of degradation also varied shifting toward higher temperatures from 399 °C for the pine to 405 °C for both coated materials. This result was found in accordance with the well-known slow decomposition of lignins over a broad temperature range [29,34] between 126 and 850 °C for this study (Fig. 2).

The "synergistic effect", ΔM, that occurred during the pyrolysis of coated materials have been illustrated by plotting the difference in weight loss between the coated material (W_{blend}) and each material in the blend, which have been weighted by their respective weight fraction, $\Sigma x_i W_i$ ($\Delta M = W_{blend} - (\Sigma x_i W_i)$). This analysis of synergistic effect, combining ΔM and DTG curves, that has been previously implemented by Cai et al. [35] and lately by Ko et al. [36], associates the negative values and $d\alpha/dt$ values close to zero with the formation of char, whereas positive values and non-null values of $d\alpha/dt$ are ascribed to interactions between volatiles. Based on this, it clearly appears that coated materials are degraded in different ways (Fig. 5). The pyrolysis of the coated material led to the formation of char occurring at two distinct stages, between 95–210 °C and 403–485 °C for LI_{20}, and between 95–162 °C and 409–492 °C for LI_{40}. The generation of the 'primary char' could be

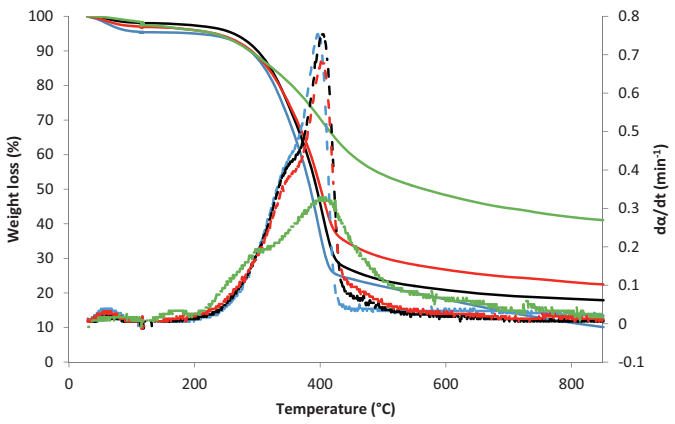

Fig. 4. Thermogravimetric and derivative curves for the raw materials (TGA ; DTG) *Pinus Radiata* and Acetocell lignin (TGA ; DTG) and the coated materials LI_{20} (TGA ; DTG) and LI_{40} (TGA ; DTG).

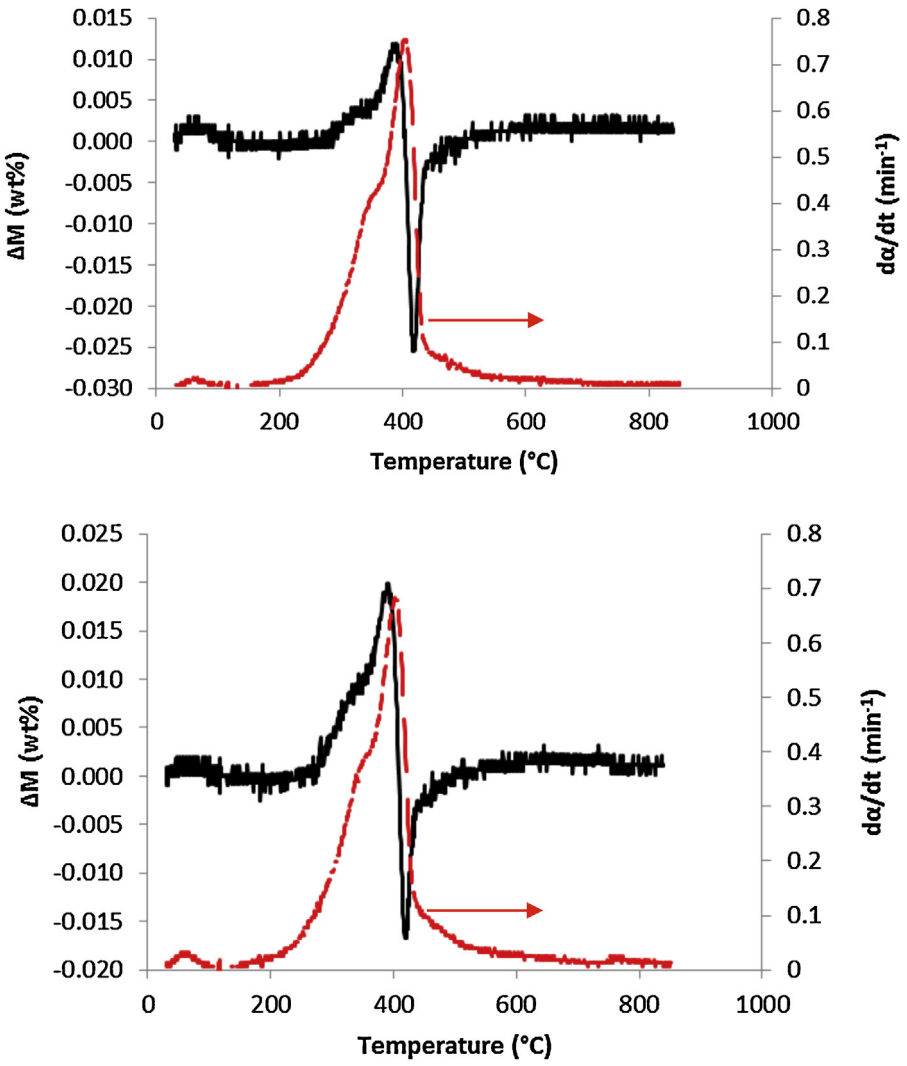

Fig. 5. Synergistic effect (ΔM) and derivated thermogravimetric curves ($d\alpha/dt$) for (a) LI_{20} and (b) LI_{40} coated materials.

attributed to (i) the dehydration of biomass and (ii) the release of volatile matter that remains retained at the interface between the biomass particle and lignin layer. Whereas the formation of the 'secondary char' may be due to (iii) reactions between highly reactive volatiles from both materials and/or (iv) the cross-linking nature of lignin.

A second synergistic event as illustrated by the positive values of ΔM appeared in both cases. Its temperature range matched perfectly that of the maximum rate of devolatilization (for $d\alpha/dt$ values above 0.4 min^{-1}), which indicates an enhanced release of volatiles when the blend is pyrolyzed. Differences in weight losses between coated materials could be then attributed to the presence and the thickness of the coating layer that varies according the preparation. Indeed, the scanning electron microscopy (SEM) images of the longitudinal and transversal sections of coated particles (Fig. 6) confirm the deposit of extracted lignin particles onto the surface of pine biomass and into its pores; thus providing an even coating over the entire surface. Also, the homogeneous and increasing brownish coloring of the coated material (Fig. 6a–d) confirmed the gradual increase of the thickness according the amount of added lignin, a second series of magnified SEM images of pores showed the gradual increase of the layer thickness (Fig. 6e). In the case of LI_{40}, the thicker layer could have then delayed the release of volatiles that underwent further chemical reactions. As a result of these chemical composition changes, apparent homogeneous synergistic effects were enhanced as judged by the comparison of calculated surface areas for LI_{40} (1.24 wt%.°C) and LI_{20} (0.62 wt%.°C) (Fig. 5b).

3.2. Fast pyrolysis of raw and coated feedstocks

3.2.1. Yields of pyrolysis product

The preparation of coated feedstock allowed the fast pyrolysis of technical lignin lowering the bio-oil yields from 47.8 wt% for pine to 42.4 wt% and 43.2 wt% for LI_{20} and LI_{40}, respectively (Table 2). This result represents a significant improvement regarding the low yields and technical issues obtained in the case of lignin [5]. It is not surprising that char yield increased as the lignin content increased. Indeed, the reactor temperature of 540 °C could have not been high enough to fully pyrolyze the lignin, which is also considered as a precursor of char [37].

The yield of organics decreased from 42.82 wt% to 31.11–32.25 wt% when the isolated lignin was added, while the pyrolytic water yield increased from 4.96 wt% to 10.97–11.27 wt% (Table 2); thus indicating that the presence of the isolated lignin affects the chemistry of pyrolysis by promoting the dehydration reactions. Although the origin of the reactive water is often attributed to the presence of intramolecular dehydration reactions occurring during the decomposition of hemicelluloses [38], it has

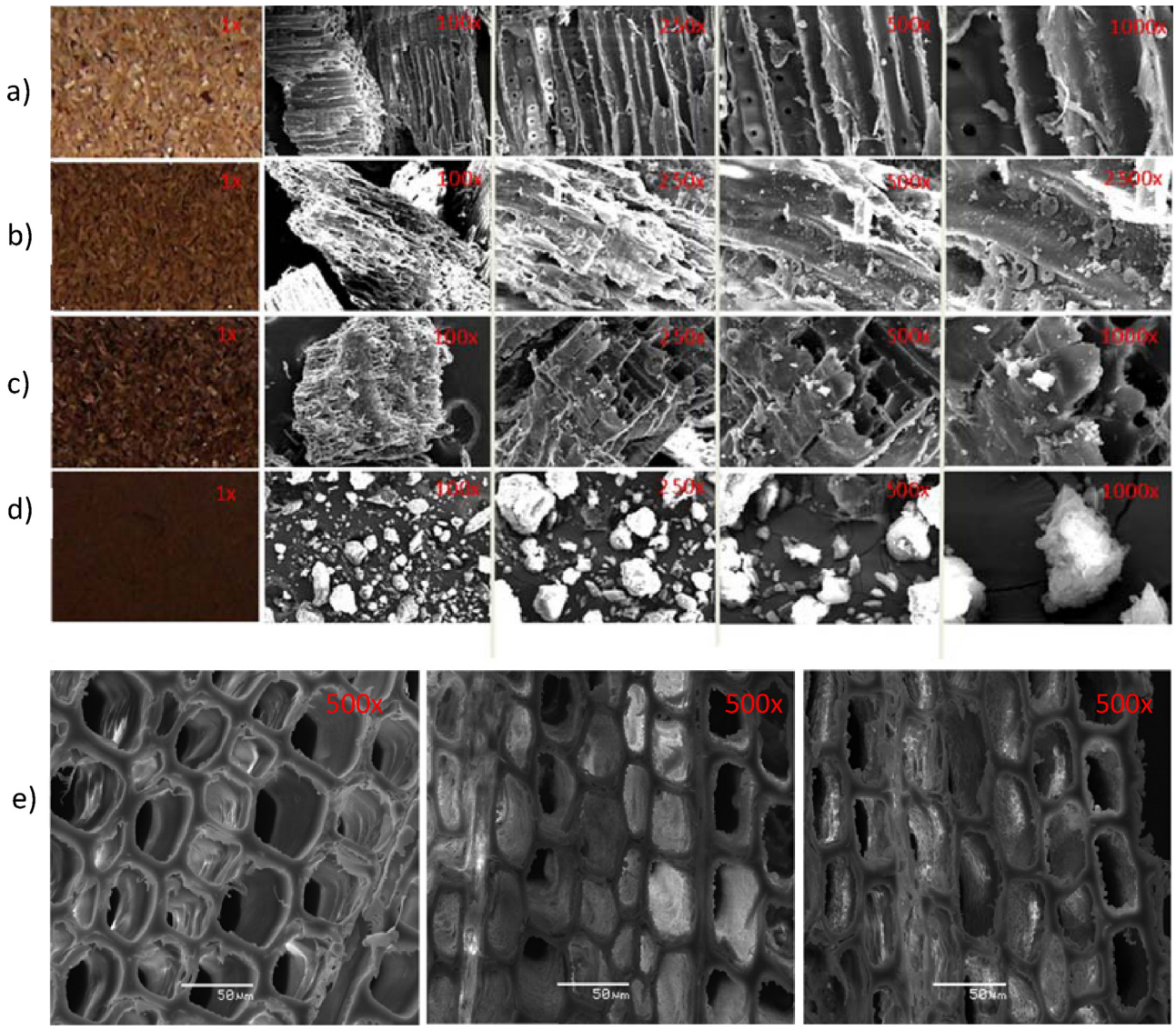

Fig. 6. SEM images of (a) Pine, (b) LI_{20}, (c) LI_{40}, (d) acid-extracted lignin powder and (e) pores of samples.

also been suggested that the covalent bonding existing between virgin lignin and hemicelluloses could significantly affect the production of pyrolytic water and organics [39]. In the present study, the substantial production of reactive water was clearly attributed to the presence of the isolated lignin.

Common views on natural polymer pyrolysis indicate that the efficient depolymerization with the production of organics is conditioned by the presence of oxygen and inter- and intramolecular hydrogen transfer reactions [40]. In this case, the low oxygen content of coating material was beneficial to the formation of liquids, whereas the nature of the extracted lignin with the presence of aliphatic and oxygenated chains and non-transferable hydrogens prevented the efficient cleavage of alkyl–aryl ether linkages leading to the substantial formation of char [41].

3.2.2. Bio-oil characterization

To better understand the chemical effect of this technical lignin on biomass pyrolysis mechanisms, the determination of the overall and partial relative product distribution and absolute concentration of key compounds were conducted.

The relative distribution of overall functional groups present in the pyrolysis bio-oils was determined via ^{13}C NMR (Fig. 7). Significant differences between the composition of bio-oils were found. If the integration results for pine were found in line with previous works [42], the addition of the isolated lignin led to an increased formation of aliphatics, by 29% for LI_{40} and 36% for LI_{20} in comparison to the initial percentage obtained for the pine (Fig. 7). Opposite trends were observed with respect to total aromatics (Aromatic C—O, aromatic C—C and aromatic C—H) with the decrease

Table 2
Yield (Y) in db, wt% from fast pyrolysis experiments.

	Y_{oil} (db, wt%)	Y_{char} (wt%)	Y_{gas^*}	$Y_{organics}$	$Y_{pyrolytic\ water}$	Y_{BOC}	Y_{BOP}	Ratio BOP:BOC
Pine	47.78 ± 4.41	9.68 ± 0.28	42.55 ± 4.59	42.82 ± 4.03	4.96 ± 0.51	35.0 ± 3.7	17.3 ± 0.2	0.50 ± 0.05
LI_{20}	42.38 ± 1.47	17.79 ± 4.79	39.84 ± 3.32	31.1 ± 1.4	11.27 ± 0.06	26.4 ± 3.3	19.8 ± 1.9	0.76 ± 0.17
LI_{40}	43.22 ± 6.47	18.87 ± 7.74	37.90 ± 1.26	32.25 ± 2.98	10.97 ± 3.49	23.7 ± 6.0	24.6 ± 7.3	1.03 ± 0.04

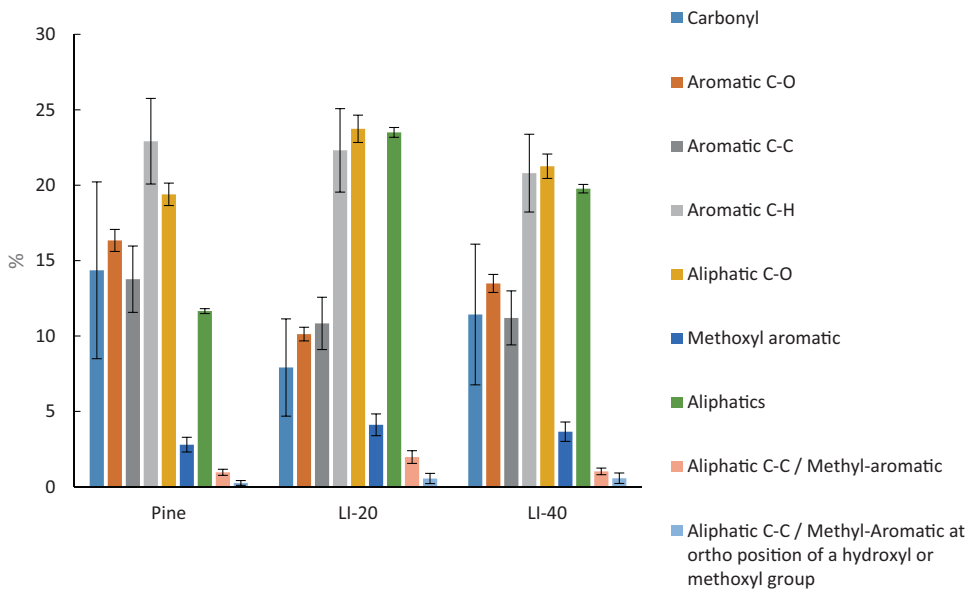

Fig. 7. Relative percentages of functional groups determined by ^{13}C NMR for the BOP fraction.

of total aromatics between 18% for LI_{40} and 23% for LI_{20}. The slight decrease in the relative percentage of oxygenated aromatics may be explained by the addition of lignin of lower oxygen content (Table 1).

The preparation of coated biomass with increasing lignin did not increase the relative abundance of total aromatics as expected, but instead increased that of aliphatics, confirming that the hydrogens limited to the aliphatic and oxygenated side chains and aromatic rings of the technical lignin were not transferred to prevent the formation of char [43], but instead could activate the release of the same aliphatic and oxygenated chains (Figs. 2 and 3).

Despite detecting only a portion of the bio-oil composition [15], the relevant chromatographic peaks were combined by chemical families to visualize changes between the relative functional group distribution with increasing amount of technical lignins. The organics were classified into thirteen groups including alcohols, ketones, aldehydes, acids, furans, compounds with a ring of 5 carbons (5-Cs), esters, anhydrosugars, phenolics, guaiacols, benzaldehydes and others (Fig. 8a–c). In this case, the GC–MS technique allowed the analysis of both liquids. The first fraction recovered from the first condensation stage via indirect cooling contact at 4 degrees contains many light oxygenated compounds (Fig. 8a) and a

Table 3
Product concentration in BOC and BOP fractions.

	Unit	Pine		LI_{20}		LI_{40}	
		BOC	BOP	BOC	BOP	BOC	BOP
Hydroxyacetaldehyde (Glycoaldehyde)	wt%, bio-oil	9.3	2.21	5.86	2.21	5.8	2.18
	wt%, dry bio-oil	7.54*		5.19*		5.88*	
	wt%, dry feed	0.080		0.065		0.076	
Acetic acid	wt%, bio-oil	3.95	2.77	3.19	3.33	**3.3**	3.47
	wt%, dry bio-oil	4.16*		5.19*		5.88*	
	wt%, dry feed	0.044		0.047		0.053	
2-propanone, 1-hydroxy (Acetol)	wt%, bio-oil	4.13	1.23	2.72	1.7	1.79	1.06
	wt%, dry bio-oil	3.26		3.68		2.78	
	wt%, dry feed	0.034		0.033		0.025	
Furfural	wt%, bio-oil	0.12	0.29	0.11	0.46	0.09	0.34
	wt%, dry bio-oil	0.25		0.39		0.26	
	wt%, dry feed	0.0027		0.0034		0.0024	
Levoglucosan	wt%, bio-oil	0.275	6.00	0.19	7.77	0.12	6.73
	wt%, dry bio-oil	4.09		4.98		3.53	
	wt%, dry feed	0.043		0.045		0.032	
Phenol	wt%, bio-oil	0.03	0.16	0.07	0.38	0.03	0.26
	wt%, dry bio-oil	0.137		0.300		0.171	
	wt%, dry feed	0.0015		0.0027		0.0015	
Phenol, 4-methyl	wt%, bio-oil	0	0.1	0	0.21	0	0.1
	wt%, dry bio-oil	0.019		0.1000		0.022	
	wt%, dry feed	0.0002		0.00090		0.00020	
Phenol, 2-methoxy-4-methyl	wt%, bio-oil	0.07	0.6	0.02	0.55	0.06	0.89
	wt%, dry bio-oil	0.427		0.359		0.529	
	wt%, dry feed	0.0045		0.0034		0.0048	

* Significantly different Student's *t*-test at 95% confidence.

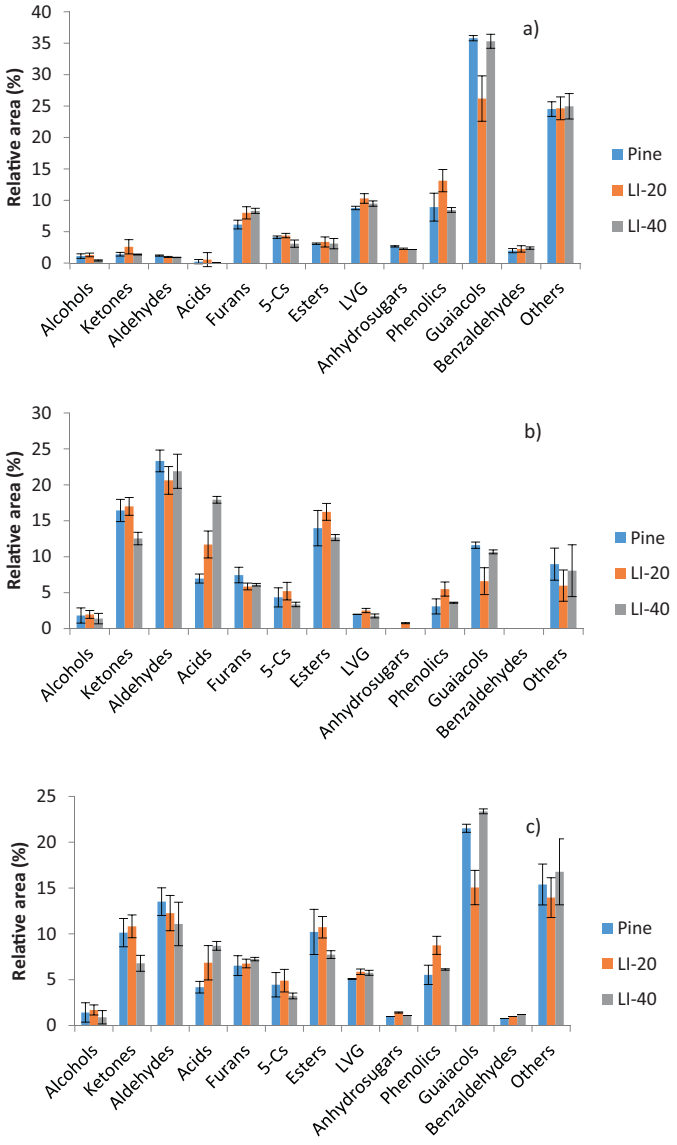

Fig. 8. Relative percentage of product distribution for (a) the BOC fraction, (b) the BOP fraction and (c) combined fractions.

large amount of water content between 33 and 38 wt%. On the other hand, the tarry phase with a lower water content in the range of 4.8–6.3 wt% collected from the second condensation stage via an electroprecipitator contains a large aromatic portion (Fig. 7) that is partially composed of phenolics and guaiacols (Fig. 8b). Although GC/MS only detects the volatiles and monomeric phenolics and not dimers, trimers, tetramers, it was observed that the addition of lignin affected the chemical composition of both aqueous and organic fractions (Fig. 8a–c).

For example, the acids content in aqueous phase increased gradually and significantly with the addition of technical lignin (Fig. 8c), trend that was corroborated by the significant increase of the aliphatic fraction depicted by the ^{13}C NMR analysis (Fig. 7) and the quantification of acetic acid concentration (Table 3). This result was attributed to the degradation of the saturated aliphatic and oxygenated side-chains into light compounds (e.g., acetic acid and water).

However, the changes with respect to other organics, in particular for phenolics and guaiacols that could not be depicted by the ^{13}C NMR analysis, did not follow a gradual trend in accordance with the increasing addition of lignin (Fig. 8). In the case of LI_{20}, an expected increase in phenolics that corresponded to a significant decrease in guaiacols was observed (Fig. 8b). While the addition of a larger amount in lignin reversed the trends up to displaying a similar functional groups distribution than that of the uncoated material for the tarry phase (Fig. 8b).

The significant increase in the phenolics accompanied with the decrease in guaiacols is not surprising, as the formation of monomeric phenolic compounds via free radical reactions has been often reported during the pyrolysis of isolated and native lignins [41,43]. In addition, the careful revision of the products separated by the GC–MS and of their MS spectrum led us to point out the presence of a phthalate ester with base peaks of *m/z* 207, 149 and 104 [44]; thus indicating that the phenols could have been further degraded in phthalate esters through the reactions of benzene radical, carbon dioxide and other alkyl radicals [45,46]. Finally, the drastic change in chemical composition of aromatics between LI_{20} and LI_{40} was attributed to the thicker layer of lignin, which prevented/slowed down the release of volatiles as mentioned in Section 3.1. The same layer could have prevented the guaiacols to be further degraded into phenols and catechols and subsequently into phthalates, reaction that was reported to occur in a gas phase [46].

The determination of absolute concentration of key organics involved into the biomass pyrolysis was also carried out. The selection of the key compounds was based on previous studies that described in detail the pyrolysis mechanisms of major polymers that composed the lignocellulosic biomass (i.e., hemicelluloses, cellulose and lignin) [38,47,48]. As a result levoglucosan (LVG), acetol (AC) and glycoaldehyde (GA) were selected to follow the cellulose pyrolysis, while phenol, phenol, 4-methyl and phenol, 2-methoxy-4-methyl were chosen as lignin-derived products. The concentrations expressed on a weight basis of dry feed of cellulose-derived products, LVG, AC and GA, remained the same or decreased with the addition of lignin (Table 3). When a gradual decrease in the carbohydrate-derived products could have been expected considering the lower proportion in carbohydrates to be pyrolyzed, the pyrolysis of LI_{20} led to higher levels in furfural and acetol in comparison to LI_{40}.

The trends observed for the lignin-derived products (i.e., phenol, phenol, 4-methyl and Phenol, 2-methoxy-4-methyl) levels, with an increasing production of phenols and a decreasing formation of guaiacols for LI_{20} were found in accordance with the functional group distribution (Fig. 8). These results indicate that the decomposition of ether bond in lignin was more efficient in the case of small addition of technical lignin, while the addition of a larger amount have led to the formation of more stable guaiacols. If the guaiacols and phenolics are often reported as main decomposition products of aryl–ether bonds, guaiacols are further converted into catechols with increasing temperature [24]; thus confirming the higher thermal stability of some guaiacols.

The levels of acetic acid increased significantly with the increase of lignin content (Table 3), suggesting that the additional amount of acid formed originates from acetoxy groups present in the isolated lignin, thus supporting the speculative free-radical chain reaction proposed by Shen et al. [46]. It is noteworthy that the acetic acid is a catalyst for oligomerizing phenolic compounds that could be formed via recombination/re-oligomerization of the primary pyrolysis products of lignin during the condensation process [38]. It is then suspected that the sufficient levels of acetic acid produced during the fast pyrolysis of LI_{40} could have promoted the oligomerization of phenolic compounds, thus lowering their content (Fig. 8c). This observation supports the reoligomerization model through radical mechanisms [14] for the formation of phenolic oligomer instead of the thermal-mechanical ejection [49].

4. Conclusions

This work has demonstrated the possibility of fast pyrolyzing a problematic feedstock, a purified lignin, with *P. radiata* sawdust. To do this, a new coating preparation method was developed. This technique consists in a wet impregnation technique, mixing the extracted lignin powder already dissolved in acetone with *P. radiata* sawdust. Conventional fast pyrolysis of the coated material was carried out at 540 °C using a fluidized bed reactor. Although a slight decrease in total liquid and organic yields were observed when both coated materials, LI_{20} and LI_{40}, were pyrolyzed, no technical issues such as bed agglomeration, feeding plugs or solid entrainment occurred. As the lignin addition increased, char, pyrolytic water yields and acids content increased. These changes were attributed to the presence of aliphatic and oxygenated side-chains within the isolated lignin's structure.

The thermal evaluation of coated materials and the in-depth characterization of both raw materials and fast pyrolysis bio-oils helped us to point out drastic mechanistic changes during the fast pyrolysis in the specific case of LI_{40}. These changes were associated with the presence of the thick layer preventing the release of pyrolysis volatiles. It was also proposed that the substantial formation of acetic acid could have catalyzed re-oligomerization reactions lowering the content in monomeric phenolics.

Acknowledgements

The authors would like to acknowledge the financial support from the Project Basal PFB-27 and the Program PMI InEs UCO-1302 of the Chilean Ministry of Education. Ms. Karen Lyssette Bustamante Tassara (CESMI) is acknowledged for performing the NMR analyses.

References

[1] P.J. De Wild, W.J.J. Huijgen, R.J.A. Gosselink, Lignin pyrolysis for profitable lignocellulosic biorefineries, Biofuels Bioprod. Biorefining 8 (2014) 645–657.
[2] R.J.a. Gosselink, E. de Jong, B. Guran, A. Abächerli, Co-ordination network for lignin – standardisation, production and applications adapted to market requirements (EUROLIGNIN), Ind. Crops Prod. 20 (2004) 121–129.
[3] J. Zakzeski, P.C. Bruijnincx, A.L. Jongerius, B.M. Weckhuysen, The catalytic valorization of lignin for the production of renewable chemicals, Chem. Rev. 110 (2010) 3552–3599.
[4] P. de Wild, H. Reith, E. Heeres, Biomass pyrolysis for chemicals, Biofuels 2 (2011) 185–208.
[5] D.J. Nowakowski, A.V. Bridgwater, D.C. Elliott, D. Meier, P. de Wild, Lignin fast pyrolysis: results from an international collaboration, J. Anal. Appl. Pyrolysis 88 (2010) 53–72.
[6] S. Feng, S. Cheng, Z. Yuan, M. Leitch, C. Xu, Valorization of bark for chemicals and materials: a review, Renew. Sustain. Energy Rev. 26 (2013) 560–578.
[7] P. Case, C. Bizama, C. Segura, M. Clayton Wheeler, A. Berg, W.J. DeSisto, Pyrolysis of pre-treated tannins obtained from radiata pine bark, J. Anal. Appl. Pyrolysis 107 (2014) 250–255.
[8] I. Wilkomirsky, E. Moreno, A. Berg, Bio-oil production from biomass by flash pyrolysis in a three-stage fluidized bed reactors system, Proceedings (2014) 6–10.
[9] S. Xiu, A. Shahbazi, Bio-oil production and upgrading research: a review, Renew. Sustain. Energy Rev. 16 (2012) 4406–4414.
[10] D. Dondi, A. Zeffiro, A. Speltini, C. Tomasi, D. Vadivel, A. Buttafava, The role of inorganic sulfur compounds in the pyrolysis of Kraft lignin, J. Anal. Appl. Pyrolysis 107 (2014) 53–58.
[11] P. Sannigrahi, A.J. Ragauskas, Fundamentals of biomass pretreatment by fractionation, in: C.E. Wyman (Ed.), Aqueous Pretreatment of Plant Biomass for Biological and Chemical Conversion to Fuels and Chemicals, first ed., John Wiley & Sons, 2013, pp. 201–222.
[12] S.H. Beis, S. Mukkamala, N. Hill, J. Joseph, C. Baker, B. Jensen, E.A. Stemmler, M.C. Wheeler, B.G. Frederick, A. van Heiningen, A.G. Berg, W.J. DeSisto, Fast pyrolysis of lignins, BioResources 5 (2010) 1408–1424.
[13] P.R. Patwardhan, Understanding the product distribution from biomass fast pyrolysis (Ph.D. thesis), Iowa State University, 2010.
[14] X. Bai, K.H. Kim, R.C. Brown, E. Dalluge, C. Hutchinson, Y.J. Lee, D. Dalluge, Formation of phenolic oligomers during fast pyrolysis of lignin, Fuel 128 (2014) 170–179.
[15] D. Mohan, C.U. Pittman, P.H. Steele, Pyrolysis of wood/biomass for bio-oil: a critical review, Energy Fuels 20 (2006) 848–889.
[16] P.J. de Wild, W.J.J. Huijgen, H.J. Heeres, Pyrolysis of wheat straw-derived organosolv lignin, J. Anal. Appl. Pyrolysis 93 (2012) 95–103.
[17] Y. Lin, C. Zhang, M. Zhang, J. Zhang, Deoxygenation of bio-oil during pyrolysis of biomass in the presence of CaO in a fluidized-bed reactor, Energy Fuels 24 (2010) 5686–5695.
[18] M. Carrier, N. Müller, H. Grandon, C. Segura, I. Wilkomirsky, A. Berg, Depolymerization of acetosolv lignin through in-situ catalytic fast pyrolysis, Rev. la Fac. Cienc. Quím. Univ. Cuenca 10 (2014) 61–66.
[19] D. Li, C. Briens, F. Berruti, Improved lignin pyrolysis for phenolics production in a bubbling bed reactor – effect of bed materials, Bioresour. Technol. 189 (2015) 7–14.
[20] A. Berg, C. Fuentealba, J. Salazar, Separation of lignocellulosic components in acetic acid media and evaluation of applications, J. Sci. Technol. For. Prod. Process. 3 (2014) 27–32.
[21] B.W. Jones, R. Venditti, S. Park, H. Jameel, B. Koo, Enhancement in enzymatic hydrolysis by mechanical refining for pretreated hardwood lignocellulosics, Bioresour. Technol. 147 (2013) 353–360.
[22] A. Sluiter, R. Ruiz, C. Scarlata, J. Sluiter, D. Templeton, Determination of extractives, in: Biomass Laboratory Analytical Procedure (LAP), NREL, 2008, pp. 1–9.
[23] C. Fernández-Costas, S. Gouveia, M.A. Sanromán, D. Moldes, Structural characterization of Kraft lignins from different spent cooking liquors by 1D and 2D Nuclear Magnetic Resonance spectroscopy, Biomass Bioenergy 63 (2014) 156–166.
[24] H. Ben, A.J. Ragauskas, NMR characterization of pyrolysis oils from Kraft lignin, Energy Fuels 25 (2011) 2322–2332.
[25] J. Meng, J. Park, D. Tilotta, S. Park, The effect of torrefaction on the chemistry of fast-pyrolysis bio-oil, Bioresour. Technol. 111 (2012) 439–446.
[26] H.J. Park, Y.-K. Park, J.S. Kim, Influence of reaction conditions and the char separation system on the production of bio-oil from radiata pine sawdust by fast pyrolysis, Fuel Process. Technol. 89 (2008) 797–802.
[27] A. Oasmaa, Y. Solantausta, V. Arpiainen, E. Kuoppala, K. Sipilä, Fast pyrolysis bio-oils from wood and agricultural residues, Energy Fuels 24 (2010) 1380–1388.
[28] S.-H. Jung, M.-H. Cho, B.-S. Kang, J.-S. Kim, Pyrolysis of a fraction of waste polypropylene and polyethylene for the recovery of BTX aromatics using a fluidized bed reactor, Fuel Process. Technol. 91 (2010) 277–284.
[29] M. Carrier, A. Loppinet-Serani, D. Denux, J.-M. Lasnier, F. Ham-Pichavant, F. Cansell, C. Aymonier, Thermogravimetric analysis as a new method to determine the lignocellulosic composition of biomass, Biomass Bioenergy 35 (2011) 298–307.
[30] C. Zhou, W. Jiang, B.K. Via, O. Fasina, G. Han, Prediction of mixed hardwood lignin and carbohydrate content using ATR–FTIR and FT–NIR, Carbohydr. Polym. 121 (2015) 336–341.
[31] S. Kubo, J.F. Kadla, Hydrogen bonding in lignin: a Fourier transform infrared model compound study, Biomacromolecules 6 (2005) 2815–2821.
[32] A. Tejado, C. Peña, J. Labidi, J.M. Echeverria, I. Mondragon, Physico-chemical characterization of lignins from different sources for use in phenol-formaldehyde resin synthesis, Bioresour. Technol. 98 (2007) 1655–1663.
[33] W. Glasser, R. Jain, Lignin derivatives. I. Alkanoates, Holzforschung 47 (1993) 225–233.
[34] E. Jakab, O. Faix, F. Till, Thermal decomposition of milled wood lignins studied by thermogravimetry/mass spectrometry, J. Anal. Appl. Pyrolysis 40–41 (1997) 171–186.
[35] J. Cai, Y. Wang, L. Zhou, Q. Huang, Thermogravimetric analysis and kinetics of coal/plastic blends during co-pyrolysis in nitrogen atmosphere, Fuel Process. Technol. 89 (2008) 21–27.
[36] K.-H. Ko, A. Rawal, V. Sahajwalla, Analysis of thermal degradation kinetics and carbon structure changes of co-pyrolysis between macadamia nut shell and PET using thermogravimetric analysis and 13C solid state nuclear magnetic resonance, Energy Convers. Manag. 86 (2014) 154–164.
[37] T. Hosoya, H. Kawamoto, S. Saka, Cellulose–hemicellulose and cellulose–lignin interactions in wood pyrolysis at gasification temperature, J. Anal. Appl. Pyrolysis 80 (2007) 118–125.
[38] P.R. Patwardhan, R.C. Brown, B.H. Shanks, Product distribution from the fast pyrolysis of hemicellulose, ChemSusChem 4 (2011) 636–643.
[39] M. Carrier, J.-E. Joubert, S. Danje, T. Hugo, J. Görgens, J.H. Knoetze, Impact of the lignocellulosic material on fast pyrolysis yields and product quality, Bioresour. Technol. 150 (2013) 129–138.
[40] T. Kotake, H. Kawamoto, S. Saka, Mechanisms for the formation of monomers and oligomers during the pyrolysis of a softwood lignin, J. Anal. Appl. Pyrolysis 105 (2014) 309–316.
[41] T. Hosoya, H. Kawamoto, S. Saka, Secondary reactions of lignin-derived primary tar components, J. Anal. Appl. Pyrolysis 83 (2008) 78–87.
[42] H. Ben, A.J. Ragauskas, Comparison for the compositions of fast and slow pyrolysis oils by NMR characterization, Bioresour. Technol. 147 (2013) 577–584.
[43] T. Hosoya, H. Kawamoto, S. Saka, Pyrolysis gasification reactivities of primary tar and char fractions from cellulose and lignin as studied with a closed ampoule reactor, J. Anal. Appl. Pyrolysis 83 (2008) 71–77.
[44] P. Yin, H. Chen, X. Liu, Q. Wang, Y. Jiang, R. Pan, Mass spectral fragmentation pathways of phthalate esters by gas chromatography–tandem mass spectrometry, Anal. Lett. 47 (2014) 1579–1588.
[45] F. Zeng, W. Liu, H. Jiang, H.-Q. Yu, R.J. Zeng, Q. Guo, Separation of phthalate esters from bio-oil derived from rice husk by a basification–acidification process and column chromatography, Bioresour. Technol. 102 (2011) 1982–1987.

[46] D.K. Shen, S. Gu, K.H. Luo, S.R. Wang, M.X. Fang, The pyrolytic degradation of wood-derived lignin from pulping process, Bioresour. Technol. 101 (2010) 6136–6146.
[47] P.R. Patwardhan, D.L. Dalluge, B.H. Shanks, R.C. Brown, Distinguishing primary and secondary reactions of cellulose pyrolysis, Bioresour. Technol. 102 (2011) 5265–5269.
[48] A.M. Azeez, D. Meier, J. Odermatt, T. Willner, Fast pyrolysis of African and European lignocellulosic biomasses using Py-GC/MS and fluidized bed reactor, Energy Fuels 24 (2010) 2078–2085.
[49] A.R. Teixeira, K.G. Mooney, J.S. Kruger, C.L. Williams, W.J. Suszynski, L.D. Schmidt, D.P. Schmidt, P.J. Dauenhauer, Aerosol generation by reactive boiling ejection of molten cellulose, Energy Environ. Sci. 4 (2011) 4306–4321.